^{1}H MR Metabolomic characterization of ovarian serous carcinoma effusions: chemotherapy-related effects and comparison with malignant mesothelioma and breast carcinoma

Riyas Vettukattil, MBBS, MMST[1], Thea Eline Hetland, MD[2], Vivi Ann Flørenes, PhD[3], Janne Kærn, MD PhD[2], Ben Davidson, MD PhD[3,4], Tone F. Bathen PhD [1]

Running title: Metabolomics of malignant effusions

[1]Dept. of Circulation and Medical Imaging, Faculty of Medicine, Norwegian University of Science and Technology (NTNU), 7491 Trondheim, Norway

[2]Departement of Gynecologic Oncology, Oslo University Hospital, Norwegian Radium Hospital, N-0424 Oslo, Norway

[3]Division of Pathology, Oslo University Hospital, Norwegian Radium Hospital, N-0424 Oslo, Norway

[4]University of Oslo, Faculty of Medicine, Institute of Clinical Medicine, N-0424 Oslo, Norway

Disclosure of funding: This work was supported by the Inger and John Fredriksen Foundation for Ovarian Cancer Research

Conflicts of interest: The authors have no personal financial or institutional interest in any of the drugs, materials, or devices described in this article.

Corresponding author:

Riyas Vettukattil
Norwegian University of Science and Technology
Faculty of Medicine
Dept. of Circulation and Medical Imaging
Postbox 8905, 7491 Trondheim, Norway
Phone: +4773598811
Fax: +4773551350
E-mail: muhammad.r.vettukattil@ntnu.no

Abstract

Malignant serous effusions are a common manifestation of advanced cancer, associated with significant morbidity and mortality. The aim of this study was to identify the metabolic differences between ovarian serous carcinoma effusions obtained pre- and post-chemotherapy, as well as to compare ovarian carcinoma (OC) effusions with breast carcinoma and malignant mesothelioma specimens. The supernatants of 115 effusion samples were analyzed by high-resolution magnetic resonance (MR) spectroscopy *in vitro* and multivariate analysis. The samples comprised of pleural and peritoneal effusions from 95 OC, 10 breast carcinomas, and 10 malignant mesotheliomas. Among the OC, 8 were paired peritoneal specimens obtained pre- and post-chemotherapy from the same patient. OC had elevated levels of ketones (aceto-acetate and beta-hydroxybutyrate) and lactate compared to malignant mesotheliomas and breast carcinomas, whereas the latter had more glucose, alanine, and pyruvate. Multivariate analysis of paired effusions in OC showed a significant increase in glucose and lipid levels in the post-treatment spectra (P=0.039). MR spectroscopy is a promising technique for comprehensive and comparative studies of metabolites in malignant serous effusions and our study shows that small metabolites associated with effusions might improve our understanding of tumor biology and disease progression and has diagnostic potential in this differential diagnosis.

Keywords: Metabolomics; Biomarkers; Magnetic Resonance Spectroscopy; Differential diagnosis; Chemotherapy; malignant effusions

1. Introduction

The accumulation of malignant effusions is a common event in clinical practice. Effusions containing tumor cells may accumulate within the serosal cavities, i.e. the peritoneal, pleural and pericardial cavity in practically every cancer type. In adults, the most common organs of origin are the breast, lung and ovary, with gastrointestinal cancers as an additional relatively common origin, especially in Asian countries. In addition to metastases, the serosal cavities are the site of origin of several cancers, including malignant mesothelioma and primary peritoneal carcinoma, although these are by far outnumbered by metastatic cancer. The finding of cancer cells in effusions is generally a marker of advanced-stage disease and is associated with poor survival in the majority of cases [1].

To improve our understanding of the tumor biology and to identify the clinically relevant events in serous effusions, it may be useful to study the small metabolites associated with these effusions in a comprehensive manner. Emerging metabolic profiling techniques enables simultaneous assessment of a broad range of endogenous and exogenous metabolites in a systematic manner [2,3]. This methodology, termed metabolomics, involves a high throughput analysis of small-molecular metabolites that are downstream products of preceding gene expressions and protein activity. Within systems biology, magnetic resonance (MR) metabolomics has become one of the key platforms, allowing rapid analysis of samples with minimal sample preparation.

Metabolic profiling of biofluids can provide an extensive view of changes in endogenous metabolites in monitoring cellular responses to perturbations such as normal physiology, diseases and drug treatments [4-8]. Metabolomics have been successfully used in the detection of biomarkers

associated with various clinical conditions such as detection of ovarian cancers [9-13] and in differentiating benign and malignant ascites [14] . Analysis of metabolites in biofluids as a diagnostic tool has several advantages such as non-invasive or minimally-invasive sample collection and the possibility of multiple sample collection over a time course thus making it an ideal choice for clinical studies [4]. Malignant effusions in serosal cavities represent an important source for potential metabolic markers. It may aid in understanding more about the metabolic basis behind malignant effusions, to identify novel biomarkers for diagnosis and treatment and to discover potential targets for therapy.

The aim of this study was to identify the metabolic differences between malignant serous effusions from patients with ovarian and breast carcinomas and malignant mesothelioma, in order to define tumor-specific patterns which may have a biological and diagnostic role. We further compared the metabolic profiles of ovarian carcinoma effusions obtained pre-chemotherapy at diagnosis and post-chemotherapy, most commonly at disease recurrence, this with the objective of defining metabolomic features which may be related to chemotherapy exposure and disease progression.

2. Materials and Methods

2.1 Patients and material

The supernatants of 115 effusion samples were analyzed using high-resolution magnetic resonance (MR) spectroscopy *in vitro* followed by multivariate analysis. The samples comprised of 95 OC (84 peritoneal, 11 pleural), 10 breast carcinomas (7 pleural, 2 peritoneal, 1 pericardial) and 10 malignant mesotheliomas (6 peritoneal, 4 pleural). Among the OC, 8 were paired peritoneal specimens obtained pre- and post-chemotherapy from the same patient. Specimens were submitted to the Norwegian Radium Hospital from 1999-2012. Due to their closely-linked histogenesis and phenotype, ovarian, peritoneal and tubal serous carcinomas are henceforth referred to as OC. Informed consent was obtained according to national guidelines. The study was approved by the Regional Committee for Medical Research Ethics in Norway.

OC specimens consisted of 2 groups. The first included 79 fresh non-fixed malignant peritoneal (n=68) and pleural (n=11) effusions from 62 patients with OC, 12 with primary peritoneal carcinoma, and 5 with tubal carcinoma. Forty-four effusions were obtained prior to chemotherapy administration, and 35 were obtained after chemotherapy, at interval debulking surgery or at recurrent disease. All patients received standard chemotherapy (platinum + paclitaxel). Clinicopathologic data of this cohort are detailed in **Table 1**.

The second group consisted of 8 pairs of patient-matched pre- and post-chemotherapy peritoneal effusions studied for chemotherapy-related changes in the metabolomic profile. These patients were not included in analyses for association with clinicopathologic parameters.

Effusions were submitted for routine diagnostic purposes and were processed immediately after tapping. Cell blocks were prepared using the Thrombin clot method. Diagnoses were established using morphology and immunohistochemistry. Effusion specimens were centrifuged, and

supernatants were frozen at -70°C. Smears and H&E-stained cell block sections were reviewed by a surgical pathologist experienced in cytopathology (BD).

2.2 Metabolic profiling

The samples were slowly thawed at room temperature. Aliquots of 300 µL were mixed with equal amount of buffer solution as described elsewhere[8]. Samples were then transferred to high-quality 5 mm MR tubes. The ratio between H_2O and D_2O was 90:10 in all samples.

2.3 MR experiments

The MR spectra were acquired using a Bruker Avance III 600MHz/54 mm US-Plus (Bruker Biospin, Rheinstetten, Germany) operating at 600 MHz for proton (1H), equipped with a QCI cryoprobe. All spectra were recorded in an automatic fashion using a Bruker SampleJet and the ICON-NMR software (Bruker Biospin). Proton spectra were obtained at a constant temperature of 300 K (27ºC) using a modified Carr-Purcell-Meiboom-Gill (CPMG) pulse sequence with presaturation during the relaxation delay (Bruker: cpmgpr1d) to achieve water suppression and to facilitate the detection of low molecular weight species by avoiding the large overlapped signals derived from large molecules such as proteins and lipids. The spectra were collected with 64 scans and 4 dummy scans. The acquisition time was 3.067 sec, measuring the FID via collection of 36864 complex data points resulting in a sweep width of 20.0363 ppm. A relaxation delay of 4 seconds was used, during which a presaturation of 25 Hz was applied. The receiver gain was kept at a constant value of 90.5 and the effective echo time was 80ms. The FIDs were Fourier transformed after exponential line broadening of 1 Hz. For metabolite quantification, nuclear overhauser effect spectroscopy (“noesy”, Bruker: noesygppr1d) spectra were acquired using the same parameters as CPMG with the exception of 32 scans. Measurement and processing was

done in full automation using Bruker standard automation programs controlled by ICON-NMR (along with TopSpin v3 patchlevel 3). Chemical shift was calibrated to the middle of the alanine peaks at 1.50 ppm. The spectra were peak aligned using icoshift [15]. The assignments of chemical shifts were done on the basis of previously published data [14] .

2.4 Data processing and multivariate analysis

Data analysis was performed with MATLAB (Version 7.9.0; The Math Works, Natick, MA, USA). The spectral region between 4.5–5.0 ppm was excluded to remove variation in water suppression efficiency. Spectra were normalized by setting the total spectral area to a constant value (=1) for all spectra to minimize possible differences in concentration between the samples.

Unsupervised principal component analysis (PCA) and supervised partial least squares discriminant analysis (PLS-DA) were performed using PLS_Toolbox v5.8.3 (Eigenvector Research, Manson, WA, USA). PCA reduces the dimensionality of the data and summarizes the structure of the multiple MR spectra visualized in score plots and loading profiles. The variance structure of the data is explained through linear combinations of the variables called principal components (PCs). The first PCs will be in the direction explaining most of the variance in the data set. In the score plot of the PCs, samples with a similar metabolic profile will cluster, while the corresponding loading profile displays the importance of each variable within the PC. PLS-DA is a supervised classification method which uses the class information to detect variables generating maximum separation between the classes. All statistical models were cross-validated with leave one out cross validation. The optimal model contains the number of latent variables yielding the lowest percentage of misclassification. A permutation test was performed (10000 permutations) to evaluate the significance of the difference between the classes [16].

Multilevel partial least squares discriminant analysis (ML-PLSDA) [17] was used for paired comparisons of multivariate data from ovarian cancers (n=8 pairs) to assess the treatment related changes in the metabolites. MLPLS-DA can be considered a multivariate extension of a paired t test that generates different multivariate submodels for the between-subject and within-subject variation in the data. This allows to split the variations and hence to analyze without being confounded by the other variation sources (especially when between subject variation is high).

2.5 Univariate analysis

To further validate the metabolites which are detected by MLPLS-DA, signal intensities from 1D noesy spectra (noesygppr1d) were integrated and compared by univariate analysis using PASW Statistics 17.0 (IBM, New York, USA). Wilcoxon Signed Ranks test was used in non-parametric analyses and p-values below 0.05 were considered statistical significant.

3. Results

3.1 Spectral assignment and multivariate analysis

Representative 1H MR spectra (CPMG) of ascitic fluids from patients with breast carcinoma, OC and mesothelioma are shown in **Figure 1**, and assignment of the various metabolites detected are given. In CPMG spectra, the broad signals from the macromolecules are filtered out and the narrow signals from small molecules are thus highlighted. The detected metabolites include amino acids (alanine, valine, isoleucine, histidine, and phenylalanine), members of energy metabolism (glucose, lactate, pyruvate, glutamate, aceto-acetate, beta-hydroxybutyrate (BHB)) and choline containing metabolites (phosphocholine, glycerophosphocholine).

Multivariate analysis was applied to a total of 115 spectra from 107 patients (including 8 paired samples). PCA of the samples (n=115) is shown in **Figure 2A**. OC effusion samples tapped from the peritoneal cavity clustered in the upper half of the PCA score plot while those from the pleural cavity and breast carcinomas tended to cluster in the lower half of the score plot (**Figure 2A**). Effusions from patients with peritoneal mesothelioma overlapped with the OC effusions from the peritoneal cavity. In general, malignant effusions of peritoneal origin and pleural origin were metabolically distinct and grouped in the upper and lower half of the PCA score plot, respectively. PCA of the samples were colored according to the tumor cell count in **Figure 2B**. Samples with more than 50% of tumor cells tend to cluster along PC1 axis with higher amount of lactate and lower amount of glucose independent of their anatomical origin. To further evaluate specimens from each anatomic space, samples from the pleural and peritoneal cavity were analyzed separately, and the results are shown in **Figure 3**.

PCA score plot of the peritoneal effusions (**Figure 3A**) showed a trend towards clustering. The metabolic profiles of OC were characterized by more lipids, aceto-acetate, BHB and acetone and lower amount of glucose and lactate compared to breast carcinomas and mesotheliomas. Similar and more clearer separation of OC samples was seen in the PCA of pleural fluids (**Figure 3B**) in which breast carcinoma and mesothelioma specimens had higher levels of glucose, pyruvate and lactate compared to OC. Effusions in mesotheliomas had similar metabolic compositions as in breast carcinoma, and hence both these effusions overlap in the PCA score plot (**Figures 3A and B**).

Unpaired samples among the OC group which was collected before (n=44) and after (n=35) chemotherapy from different patients did not show any significant differences in their spectral profiles. However, ML-PLSDA of paired samples showed that glucose and lipid levels in the ascitic fluid increased after treatment. There was also a reduction in the levels of lactate and BHB after treatment (**Figure 4**). A permutation test (to evaluate the significance of the difference between the classes) showed that the treatment-related metabolic changes were statistically significant (P=0.039, Sensitivity=87%, Specificity=87%).

3.2 Univariate analysis

The glucose signal intensities (integrals) before and after treatment were compared using Wilcoxon Signed Ranks test, showing an increase in glucose concentration in the post- treatment samples (P = 0.017).

4 Discussions

In this study, we explored the differences in the metabolic patterns of malignant serous effusions from patients with OC, breast carcinoma and malignant mesothelioma using high resolution 1H MR spectroscopy. There were differences in the metabolic profiles of OC effusions compared to the two other cancers. We further observed significant differences in the metabolic fingerprints of effusions from OC patients in response to chemotherapy by using the multilevel structure of the paired dataset.

Metabolic compositions of the serous effusions are reflected in the MR spectra as variations in size, shape and position of MR signals. Each metabolite appears at specific locations in the spectrum and each reflects specific cellular and biochemical processes. Effusions in metastatic carcinomas with tumor cells indicate an advanced stage of malignancy. The metabolic composition of the effusion fluid depends on factors which govern the formation of the fluid, movement of the metabolites across the compartments and the metabolic activities of the malignant cells. It is believed that the mechanisms underlying malignant effusion accumulation include lymphatic obstruction by metastatic cells impeding the outflow of peritoneal fluid, increased vascular permeability and new blood vessel formation, increased production by lining cells, changes in the peritoneal stroma and fibrin accumulation [1,18]. A major portion of the increase in vascular permeability which contributes to effusion formation is caused by malignancy-induced angiogenesis, resulting in accumulation of protein-rich fluid (a filtrate of whole blood) in the peritoneal cavity [18]. The MR spectra showed that the effusion supernatant contains a wide range of metabolites like glucose, amino acids, pyruvate, lactate, and lipids.

The observed differences in the metabolic profile of effusion fluid are dependent on the type of malignancy and the site of effusion. OC have higher levels of lipids and ketones (BHB, acetone, acetoacetate) and lower levels of glucose, alanine, pyruvate and lactate than breast carcinoma and mesothelioma effusions. Elevated levels of acetone, acetoacetate and BHB are seen in blood serum samples of early-stage ovarian cancer [10] and colorectal cancer [19]. Increase in ketones may be linked to lipolysis, which can be triggered to meet the growing energy demand by tumor cells [19]. In the process of metastasis to serous cavities, the malignant cells can remain viable while suspended in the effusion fluid, which forms a microenvironment for the tumor cells. Hence the metabolic composition of the effusion may be closely linked to the severity and invasiveness of the metastatic cells. Compared to malignant pleural effusions, the peritoneal fluids contain more lipids. The infiltration of lymphatics by malignant cells can impede the normal flow of chyle, which is rich in lipids, from the small intestine and can contribute to high lipid content in the peritoneal effusions. Samples with high cellularity (>50%) have higher amount of lactate and lower amount of glucose, which may represent high energy demand and glycolytic activity in effusions with increased tumor cells. Even though the spectra were normalized before the PCA analysis to account for the variation in metabolic concentrations between the samples, strong lactate signals in the samples can render the normalization process suboptimal. Separate analysis of pleural and peritoneal effusions (Figure 3) showed that lipids are elevated in OC compared to breast carcinoma and mesothelioma effusions, indicating that other mechanisms may also contribute to high lipid signals. Increased expression of fatty acid synthase (FAS), the enzyme responsible for *de novo* fatty acid synthesis has been observed in ovarian carcinomas [20-22]. Furthermore, inhibition of FAS has been shown to be cytotoxic to SKOV3 human ovarian cancer cells [23] and delays disease progression in drug-resistant OVCAR-3 human ovarian carcinoma in nude mice [24]. It is seen that ovarian cancers has a predilection for omental metastasis, where there

is a number of adipocytes. Transfer of fatty acids from adipocytes to metastatic cells provides energy for the cancer cells and promotes rapid tumor growth and metastasis [25]. Apolipoprotein E (ApoE), an important member of the lipid transport system is highly expressed in high grade ovarian serous carcinomas and is found to be essential for cell proliferation and survival of the ApoE expressing cancer cell line OVCAR3[26]. Lipid metabolism and transport in ovarian cancers needs further evaluation to identify potential therapeutic targets.

The metabolic profile of OC was distinct from breast carcinoma and malignant mesothelioma, which showed many overlapping features in multivariate analysis. This difference was clearer in pleural effusions than in peritoneal specimens (Figure 3B). As pleural effusion in OC represents an advanced stage of the disease (stage IV) with poor survival [27,28], the tumor cells may be metabolically more aggressive than their peritoneal counterpart. The effusions from breast carcinoma and mesotheliomas had relatively lower levels of ketones and higher levels of glucose, alanine, pyruvate and lactate than OC, probably indicating less fatty acid breakdown in these tumor cells. In metastatic effusions, effusion fluid 'feeds' the cancer cells and forms a dynamic microenvironment for exchange of nutrients and mitogenic factors [29,30]. Further exploration is necessary to understand more about the underlying mechanisms behind energy transfers in effusion fluid.

Post-chemotherapy samples showed an elevation in glucose and lipids with a reduction in BHB and lactate in the effusion. This may be due to a reduction in energy demand, reduction in number of live malignant cells or a change in tumor cell metabolism resulting in reduced glucose utilization from the microenvironment, decreased lipolysis and a reduction in BHB production. Early reduction in glucose uptake by the ovarian cancer cell line OVCAR-3 in response to

293 cisplatin treatment has been shown before [31]. Similar changes in glucose levels related to
294 chemotherapeutic agents have also been reported in other cancers, like breast carcinoma cell lines
295 [32,33] and gastrointestinal stromal tumor [34]. Hence, measuring glucose uptake by the malignant
296 cells might be useful in evaluating chemosensitivity in ovarian cancer patients. In this study, we
297 analyzed only a small number of patient-matched specimens as a pilot, precluding analysis of the
298 association between metabolic changes following treatment and clinical parameters such
299 treatment response and survival, and further studies are needed to decipher the mechanisms in
300 detail. Exploration of chemotherapy-induced changes in non-matched samples failed to detect the
301 changes. This clearly shows the importance of paired metabolomic analyses from same patient to
302 overcome high metabolic variation between subjects. Understanding the mechanisms behind
303 therapy-related metabolic changes may help in developing preventive strategies for improving the
304 prognosis of patients and merits further exploration in larger cohorts. In this study, we could
305 study only the effusion fluid and a combined metabolic analysis which includes the tumor cells
306 from patient-matched OC from different anatomic site could be an area of research that warrants
307 future study.
308

5. Conclusions

Differences in metabolic profiles of malignant serous effusion from different anatomical sites were detected, and metabolic features related to chemotherapy exposure were identified from the MR spectra. Metabolic characterization by high resolution proton MR spectroscopy could be a promising technique to further understand the mechanisms of effusion development in malignancies and to target clinical intervention.

Acknowledgments

Financial acknowledgment: This work was supported by the Inger and John Fredriksen Foundation for Ovarian Cancer Research

References

1. Davidson B, Firat P, Michael CW. *Serous effusions*. New York: Springer; 2011.

2. Zhang A, Sun H, Wang P, Han Y, Wang X. Modern analytical techniques in metabolomics analysis. *Analyst.* 2012;137(2):293-300.

3. Nicholson JK, Lindon JC. Systems biology: Metabonomics. *Nature.* 2008;455(7216):1054-1056.

4. Zhang A, Sun H, Wang P, Han Y, Wang X. Recent and potential developments of biofluid analyses in metabolomics. *J Proteomics.* 2012;75(4):1079-1088.

5. Napoli C, Sperandio N, Lawlor RT, Scarpa A, Molinari H, Assfalg M. Urine metabolic signature of pancreatic ductal adenocarcinoma by (1)h nuclear magnetic resonance: Identification, mapping, and evolution. *J Proteome Res.* 2012;11(2):1274-1283.

6. Zhang A, Sun H, Wang X. Serum metabolomics as a novel diagnostic approach for disease: A systematic review. *Anal Bioanal Chem.* 2012;404(4):1239-1245.

7. Denison FC, Semple SI, Stock SJ, Walker J, Marshall I, Norman JE. Novel use of proton magnetic resonance spectroscopy (1hmrs) to non-invasively assess placental metabolism. *PLoS One.* 2012;7(8):e42926.

8. Bye A, Vettukattil R, Aspenes ST, et al. Serum levels of choline-containing compounds are associated with aerobic fitness level: The hunt-study. *PLoS One.* 2012;7(7):e42330.

9. Zhang T, Wu X, Yin M, et al. Discrimination between malignant and benign ovarian tumors by plasma metabolomic profiling using ultra performance liquid chromatography/mass spectrometry. *Clin Chim Acta.* 2012;413(9-10):861-868.

10. Garcia E, Andrews C, Hua J, et al. Diagnosis of early stage ovarian cancer by 1h nmr metabonomics of serum explored by use of a microflow nmr probe. *J Proteome Res.* 2011;10(4):1765-1771.

11. Spiliotis J, Halkia E, Roukos DH. Ovarian cancer screening and peritoneal carcinomatosis: Standards, 'omics' and mirnas for personalized management. *Expert Rev Mol Diagn.* 2011;11(5):465-467.

12. Chen J, Zhang X, Cao R, et al. Serum 27-nor-5beta-cholestane-3,7,12,24,25 pentol glucuronide discovered by metabolomics as potential diagnostic biomarker for epithelium ovarian cancer. *J Proteome Res.* 2011;10(5):2625-2632.

13. Slupsky CM, Steed H, Wells TH, et al. Urine metabolite analysis offers potential early diagnosis of ovarian and breast cancers. *Clin Cancer Res.* 2010;16(23):5835-5841.

14. Bala L, Sharma A, Yellapa RK, Roy R, Choudhuri G, Khetrapal CL. (1)h nmr spectroscopy of ascitic fluid: Discrimination between malignant and benign ascites and comparison of the results with conventional methods. *NMR Biomed.* 2008;21(6):606-614.

15. Savorani F, Tomasi G, Engelsen SB. Icoshift: A versatile tool for the rapid alignment of 1d nmr spectra. *Journal of Magnetic Resonance.*202(2):190-202.

16. Westerhuis J, Hoefsloot H, Smit S, et al. Assessment of plsda cross validation. *Metabolomics.* 2008;4(1):81-89.

17. van Velzen EJ, Westerhuis JA, van Duynhoven JP, et al. Multilevel data analysis of a crossover designed human nutritional intervention study. *J Proteome Res.* 2008;7(10):4483-4491.

18. Garrison RN, Galloway RH, Heuser LS. Mechanisms of malignant ascites production. *J Surg Res.* 1987;42(2):126-132.

19. Ludwig C, Ward DG, Martin A, et al. Fast targeted multidimensional nmr metabolomics of colorectal cancer. *Magn Reson Chem.* 2009;47 Suppl 1:S68-73.

20. Alo PL, Visca P, Framarino ML, et al. Immunohistochemical study of fatty acid synthase in ovarian neoplasms. *Oncol Rep.* 2000;7(6):1383-1388.

21. Gansler TS, Hardman W, 3rd, Hunt DA, Schaffel S, Hennigar RA. Increased expression of fatty acid synthase (oa-519) in ovarian neoplasms predicts shorter survival. *Human Pathology.* 1997;28(6):686-692.

22. Ueda SM, Yap KL, Davidson B, et al. Expression of fatty acid synthase depends on nac1 and is associated with recurrent ovarian serous carcinomas. *J Oncol.* 2010;2010:285191.

23. Zhou W, Han WF, Landree LE, et al. Fatty acid synthase inhibition activates amp-activated protein kinase in skov3 human ovarian cancer cells. *Cancer Res.* 2007;67(7):2964-2971.

24. Pizer ES, Wood FD, Heine HS, Romantsev FE, Pasternack GR, Kuhajda FP. Inhibition of fatty acid synthesis delays disease progression in a xenograft model of ovarian cancer. *Cancer Res.* 1996;56(6):1189-1193.

25. Nieman KM, Kenny HA, Penicka CV, et al. Adipocytes promote ovarian cancer metastasis and provide energy for rapid tumor growth. *Nat Med.* 2011;17(11):1498-1503.

26. Chen YC, Pohl G, Wang TL, et al. Apolipoprotein e is required for cell proliferation and survival in ovarian cancer. *Cancer Res.* 2005;65(1):331-337.

27. Akahira JI, Yoshikawa H, Shimizu Y, et al. Prognostic factors of stage iv epithelial ovarian cancer: A multicenter retrospective study. *Gynecol Oncol.* 2001;81(3):398-403.

28. Bonnefoi H, A'Hern RP, Fisher C, et al. Natural history of stage iv epithelial ovarian cancer. *J Clin Oncol.* 1999;17(3):767-775.

29. Kassis J, Klominek J, Kohn EC. Tumor microenvironment: What can effusions teach us? *Diagnostic Cytopathology.* 2005;33(5):316-319.

30. Martinez-Outschoorn UE, Pestell RG, Howell A, et al. Energy transfer in "parasitic" cancer metabolism: Mitochondria are the powerhouse and achilles' heel of tumor cells. *Cell Cycle.* 2011;10(24):4208-4216.

31. Egawa-Takata T, Endo H, Fujita M, et al. Early reduction of glucose uptake after cisplatin treatment is a marker of cisplatin sensitivity in ovarian cancer. *Cancer Sci.* 2010;101(10):2171-2178.

32. Direcks WG, Berndsen SC, Proost N, et al. [18f]fdg and [18f]flt uptake in human breast cancer cells in relation to the effects of chemotherapy: An in vitro study. *Br J Cancer.* 2008;99(3):481-487.

33. Engles JM, Quarless SA, Mambo E, Ishimori T, Cho SY, Wahl RL. Stunning and its effect on 3h-fdg uptake and key gene expression in breast cancer cells undergoing chemotherapy. *J Nucl Med.* 2006;47(4):603-608.

34. Cullinane C, Dorow DS, Kansara M, et al. An in vivo tumor model exploiting metabolic response as a biomarker for targeted drug development. *Cancer Res.* 2005;65(21):9633-9636.

Figure Legends

Figure 1

Proton magnetic resonance spectra from malignant effusions

Assignments of various metabolites visible in the MR spectra are shown. The region between 6.9 ppm-7.9ppm is scaled up to show the assignments. The red spectrum is from breast carcinoma effusion, and the green from mesothelioma and the blue from ovarian carcinoma.

Figure 2

Principal Component Analysis of serous effusions

A) Score plot of PC1 vs PC2 of breast carcinoma, ovarian carcinoma and mesothelioma with different anatomical origin. Corresponding loading plot for PC2 shows the metabolic differences between the samples. B) Same score plot as in A with the samples colored according to their tumor content. Red samples are with <50% and green samples are with >50% tumor content.

Figure 3

Principal Component Analysis of serous effusions

Biplots of the malignant effusion from mesothelioma, breast and ovarian carcinoma. (A) Peritoneal effusions (B) Pleural effusions

Figure 4

Multi-level Analysis (MLPLSDA) of paired samples showing treatment-related changes.

Scatter plot of LV1 vs LV2 showing difference between pre-treatment and post-treatment samples. Corresponding loading plot (of LV1 vs LV2) showing the metabolites.

Figure 1

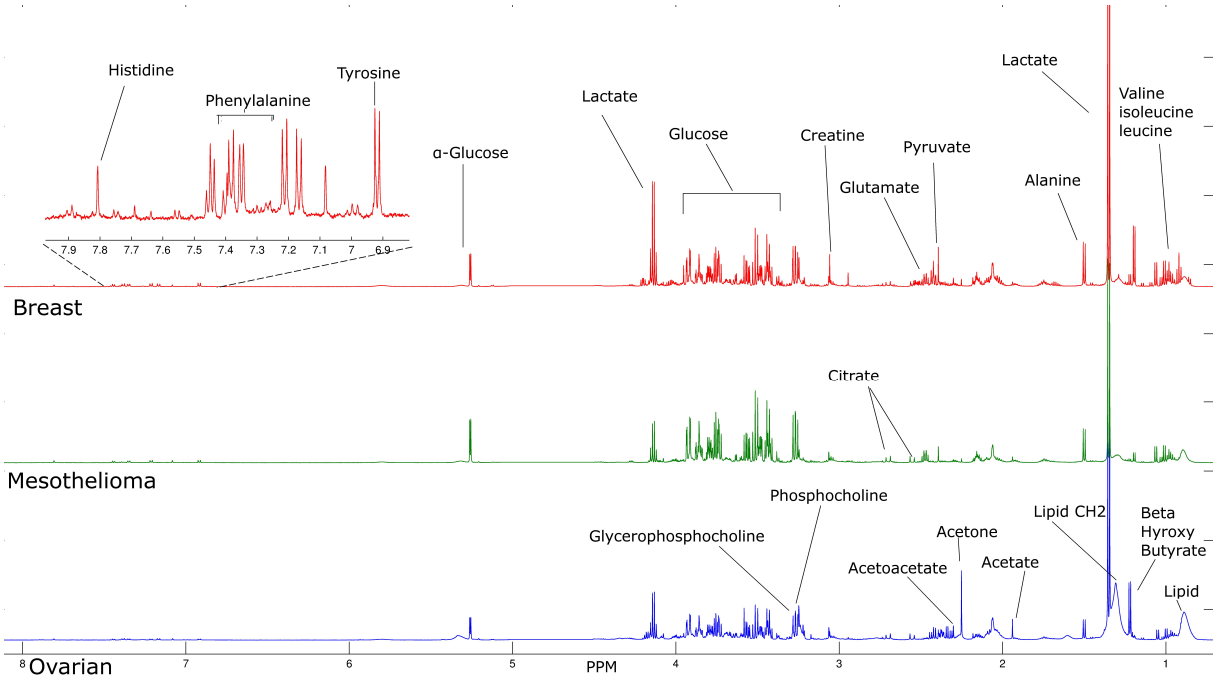

Figure 2

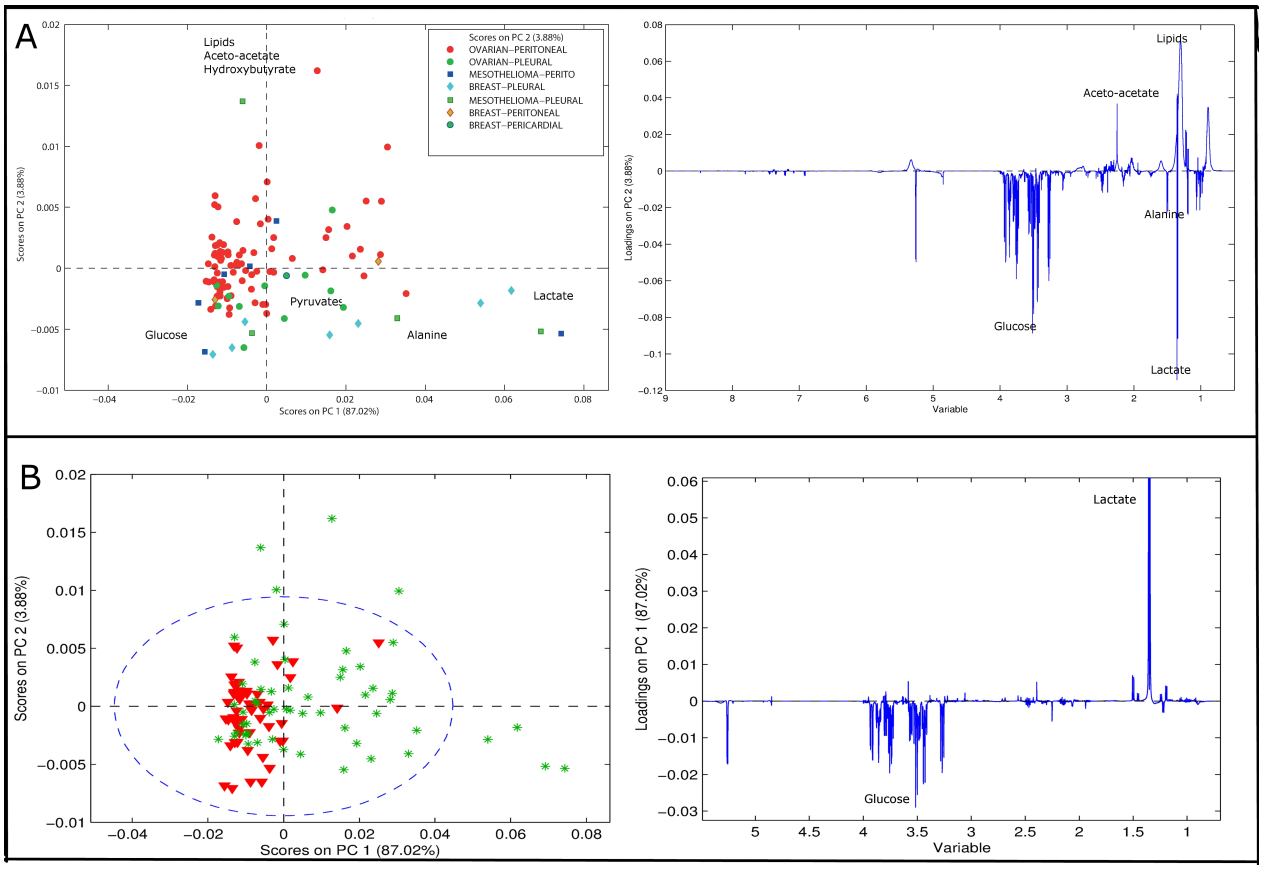

437

438 **Figure3**

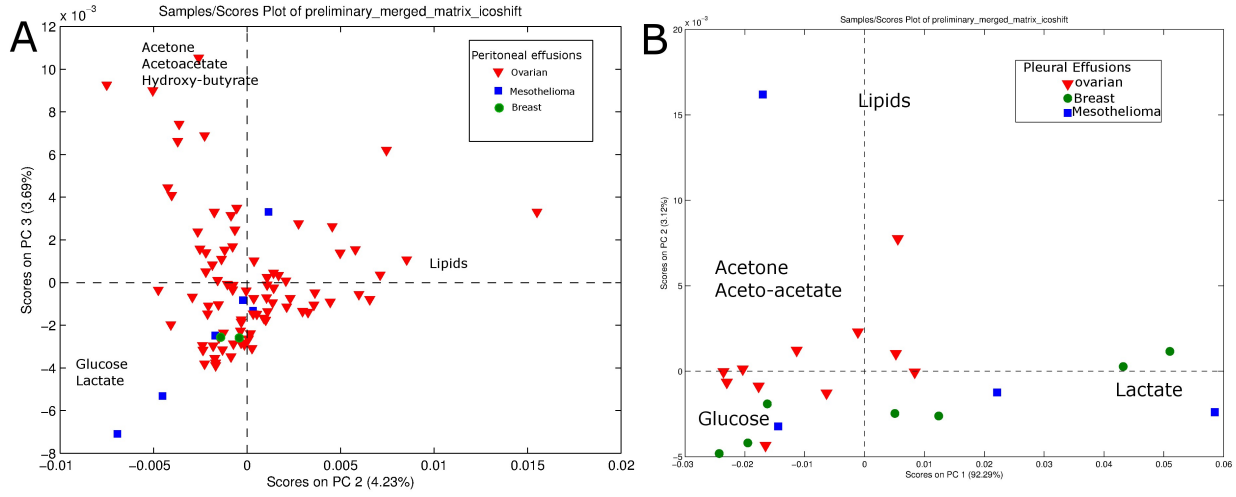

439

440

441

442

443 **Figure 4**

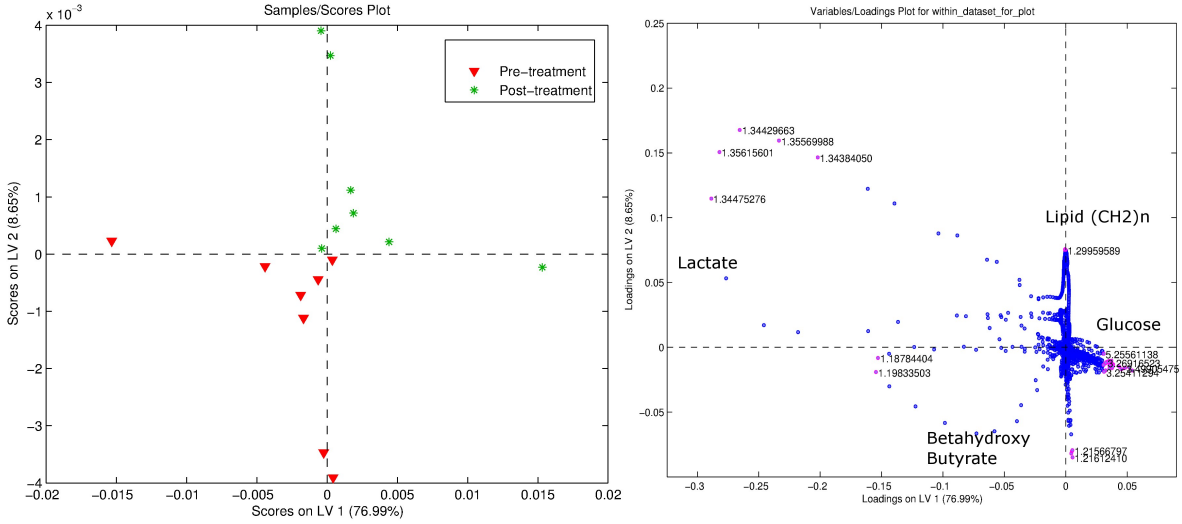

444

445

446